Merz, B., Nguyen, D., Apel, H., Gerlitz, L., Schröter, K., Steirou, E.-S., Vorogushyn, S. (2018): Spatial coherence of flood-rich and flood-poor periods across Germany. - *Journal of Hydrology*, *559*, pp. 813—826.

DOI: http://doi.org/10.1016/j.jhydrol.2018.02.082

Manuscript 26043, Journal of Hydrology

Spatial coherence of flood-rich and flood-poor periods across Germany

Authors:

Bruno Merz[1,2], Nguyen Viet Dung[1], Heiko Apel[1], Lars Gerlitz[1], Kai Schröter[1], Eva Steirou[1], Sergiy Vorogushyn[1]

[1]Section Hydrology, GFZ German Research Center for Geosciences, 14473 Potsdam, Germany
[2]Institute of Earth and Environmental Science, University of Potsdam, 14476 Potsdam, Germany

Corresponding author: Bruno Merz, bmerz@gfz-potsdam.de

Keywords: flood timing, spatial coherence, flood regimes, climate variability, catchment wetness

Abstract

Despite its societal relevance, the question whether fluctuations in flood occurrence or magnitude are coherent in space has hardly been addressed in quantitative terms. We investigate this question for Germany by analysing fluctuations in annual maximum series (AMS) values at 68 discharge gauges for the common time period 1932-2005. We find remarkable spatial coherence across Germany given its different flood regimes. For example, there is a tendency that flood-rich/-poor years in sub-catchments of the Rhine basin, which are dominated by winter floods, coincide with flood-rich/-poor years in the southern sub-catchments of the Danube basin, which have their dominant flood season in summer. Our findings indicate that coherence is caused rather by persistence in catchment wetness than by persistent periods of higher/lower event precipitation. Further, we propose to differentiate between event-type and non-event-type coherence. There are quite a number of hydrological years with considerable non-event-type coherence, i.e. AMS values of the 68 gauges are spread out through the year but in the same magnitude range. Years with

extreme flooding tend to be of event-type and non-coherent, i.e. there is at least one precipitation event that affects many catchments to various degree. Although spatial coherence is a remarkable phenomenon, and large-scale flooding across Germany can lead to severe situations, extreme magnitudes across the whole country within one event or within one year were not observed in the investigated period.

1. Introduction

The typical frame in flood hydrology is the catchment view. However, the question whether flooding is coherent beyond catchment boundaries has recently received more attention. For example, Uhlemann et al. (2010) analysed trans-basin flood events that affect many sites in different river basins simultaneously. Such events are particularly relevant for disaster management and the (re-)insurance industry. Further, it has been observed that there are flood-rich and flood-poor periods, and that periods with higher or more frequent floods can be differentiated from periods with minor flood activity (for a compilation of European studies see Hall et al., 2014). It is an interesting and societally relevant question whether such fluctuations in flood activity are coherent in space.

Spatial coherence of flood activity, i.e. the synchronous occurrence of floods in the spatial domain, can be defined in terms of flood occurrence or in terms of flood magnitude. The first approach analyses the number of flood events, either based on POT (Peak-Over-Threshold) values or using proxies. For example, Llasat et al. (2005) reconstructed annual times series composed of three classes (no flooding recorded; at least one extraordinary flooding recorded; at least two extraordinary flooding recorded). Temporal changes in flood magnitude are typically investigated by using block maxima, as e.g. annual maximum values. Both approaches can be found in the literature, whereas studies using historical data typically use flood occurrence because magnitudes of floods prior to systematic measurements are very difficult to estimate.

Several studies stressed the large spatial heterogeneity in flood activity. Mudelsee et al. (2004) found notable differences and low correlation between flood occurrence rates of the neighbouring Central European rivers Oder and Elbe for the last 800 years. Similarly, Mudelsee et al. (2006) concluded that temporal variations in flood occurrence for the period 1500-2000 in the Werra catchment in central Germany contrasted with those in the nearby Elbe catchment. Böhm and Wetzel (2006) analysed the occurrence of floods and found that flood-rich and flood-poor periods since 1300 in the adjacent catchments Isar and Lech in south Germany only partly overlapped. Annual maximum floods of 15 tributaries of the Canadian St. Lawrence River were found to correlate with different climate indices, emphasizing significant spatial heterogeneity between sub-catchments (Assani et al., 2010). The analysis of flood-rich and flood-poor periods, described in terms of the frequency of events larger than the 10-year flood, since 1850 at 83 Swiss stations showed large regional differences, especially between north and south Switzerland (Schmocker-Fackel and Naef, 2010a). In contrast, other studies stressed the spatial coherence of flood activity, even across large distances (e.g. several 100 km). Llasat et al. (2005) found coherent periods of flood occurrence in three rivers in northeast Spain since the 14th century. They concluded that the coincidence of flood-rich periods with additional catchments in the west Mediterranean region suggested a large-scale response to climatic anomalies. Schmocker-Fackel and Naef (2010b) emphasized for 14 Swiss rivers, that flood-rich periods since 1500 were often in phase with flood-rich periods in the Czech Republic, Italy and Spain, but less often with those in Germany.

Hence, the literature on spatial coherence of flood-rich and flood-poor periods provides evidences for both spatial coherence across regions and for spatial heterogeneity. This is not surprising because the studies comprise different flood indicators, methods, temporal and spatial scales, and regions. For instance, the spatial scale is important because proximity tends to favour spatial coherence. Further, the degree of spatial coherence of flood activity should vary between regions whose flood generation is governed by different processes. Regions (e.g. Australia, see Kiem et al., 2003) whose flood activity is dominated by variations of the large-scale circulation (as represented by climate teleconnections) are expected to show stronger spatial coherence compared to regions characterized by a high-frequent atmospheric variability (e.g. westerly-dominated Central Europe, see Steirou et al., 2017). However, there seems to be consensus that the degree and causes of spatial coherence of flood activity need to be better understood (Hall et al., 2014).

Floods are shaped by the interplay of processes in the atmosphere, catchment and river network, and the spatial coherence of flooding is likely a consequence of the similarity in one or several of these processes. For example, Glaser et al. (2010) investigated the flood occurrence for 20 major rivers in Central Europe and the Mediterranean region and found that the number of floods was mainly triggered by regional climate forcing with typically minor influence on adjacent catchments. However, extreme, supra-regional climatic events, such as the cold winter 1784, triggered ice-jam floods across large parts of Europe. Hence, the strength of spatial coherence is expected to vary with the flood generation processes.

The most prominent cause for spatial coherence of flood activity is climate variability. Large-scale circulation modes, such as the El Nino Southern Oscillation, influence flood characteristics at the global scale (Ward et al., 2014). Northern hemispheric pressure anomalies, e.g. the North Atlantic Oscillation, have been shown to alter the flood activity over vast parts of Europe (Steirou et al., 2017). Mesoscale synoptic weather patterns have been identified as flood drivers at the regional scale, e.g. in Germany (Petrow et al., 2009). Climate variability may modulate flood activity by changes in event meteorology, such as increased flood event precipitation. In addition, climate variability might influence the catchment wetness, leading to systematic changes in initial conditions for flood events. Since catchment wetness is also influenced by the memory of catchments, climate mechanisms and catchment characteristics may work together in shaping flood-rich and flood-poor periods. In river basins, the river network may also contribute to spatial coherence of flooding, since downstream flood peaks may result from upstream floods. Hence, far-distance locations within river networks can be linked in their flood activity.

As an example for significant spatial coherence in flood magnitude, Fig. 1 shows (smoothed) time series of annual maximum flows for nine streamflow stations in Germany for which long systematic observations are available. The stations cover Alpine rivers at the southern border of Germany with catchment areas partly in Austria (Burghausen/Salzach) and Switzerland (Neuhausen/Rhine), the middle mountain range rivers in central Germany (Cochem/Mosel, Schweinfurt/Main) and in north Germany (Vlotho/Weser), and stations along the large rivers (Cologne/Rhein, Achleiten/Danube, Dresden/Elbe). Although the set of stations covers a broad spectrum of climate and landscape characteristics and samples different flood regimes, the synchronisation between the flood time series is remarkable. The ups and downs are often parallel and periods with major flood activity tend to occur at the same time at different gauges across different basins.

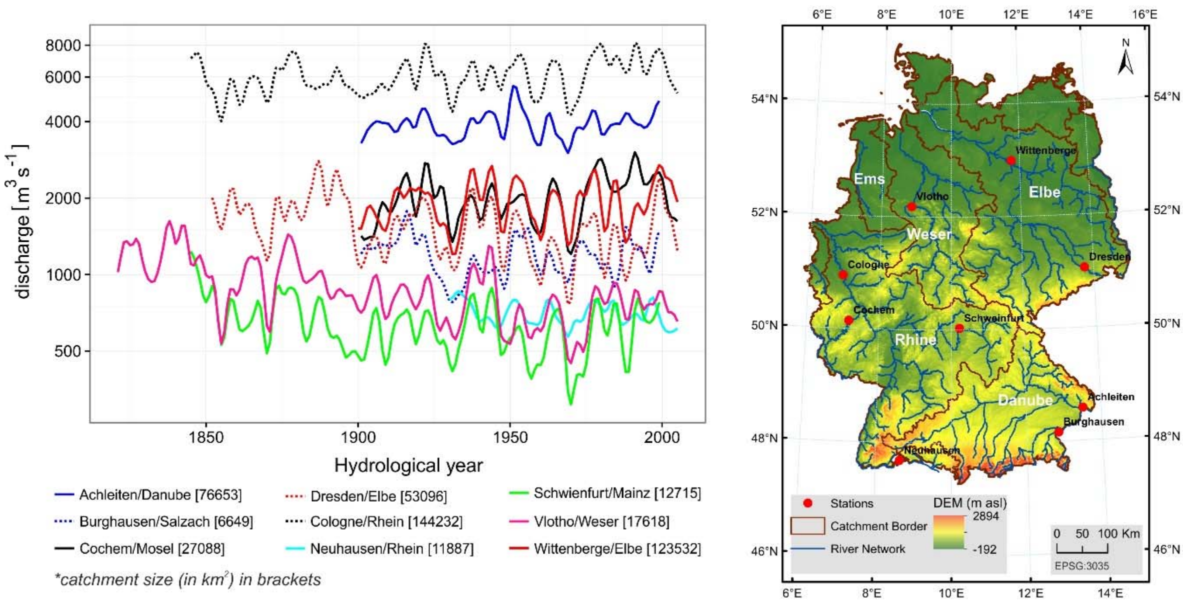

Fig. 1: Annual maximum flood time series, smoothed with a Hamming filter (Oppenheim et al., 1999) with bandwidth of seven years, for selected stations in Germany.

To better understand the degree and underlying mechanisms of synchronization of flood-rich/-poor periods, we investigate the spatial coherence in the annual maximum streamflow (AMS) across Germany, representing an area of roughly 360,000 km^2. We consider years with high spatial coherence as those years which have AMS magnitudes of the different stations in the same range, for instance, high flood peaks throughout the hydrological year. Large heterogeneity in AMS values is considered as non-coherence. By using the timing of floods, we further distinguish two types of spatial coherence (or non-coherence). Event-type coherence is given when the AMS events within a hydrological year are caused by a few flood events that impact many catchments at the same time. Hence, AMS peaks at different gauges are clustered within a few events, whereas an event may last for a few days. On the other hand, non-event-type means that the AMS values are spread throughout the year, i.e. many flood events occur during one hydrological year.

The schematic representation in Fig. 2 illustrates our understanding of spatial coherence for an artificial data set. Each sub-graph shows one hydrological year, whereas the AMS values of all gauges of this specific year are plotted versus their timing, i.e. occurrence in the year. To make the AMS values of different gauges comparable, they are standardized to zero mean and unit variance. A flood-rich and flood-poor year is given for each case. The upper left situation shows a non-event-type, coherent year. The timing of AMS values is spread throughout the year and AMS magnitudes are confined to a certain range. Non-event-type non-coherence is visualized in the upper right quadrant. AMS values occur throughout the year and AMS magnitudes vary widely, i.e. timing and magnitude vary randomly. Event-type coherence (lower left) is marked by a few events where many gauges show an AMS value at the same time, and AMS magnitudes are confined to a similar range. Event-type non-coherence (lower right) means that the AMS values are confined to a few events but AMS magnitudes vary widely.

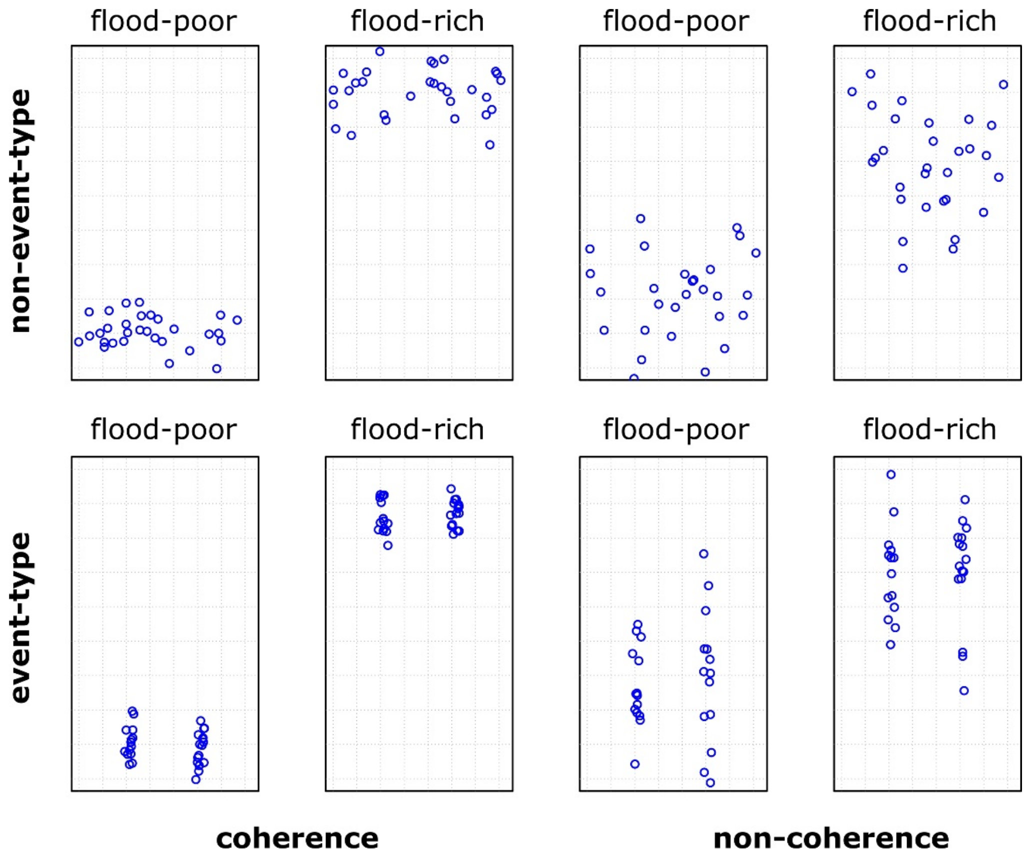

Fig. 2: Illustration of different types of AMS coherence or non-coherence using artificial data. Each graph shows the AMS values of all gauges for one specific year. Each circle marks the timing throughout the hydrological year (horizontal axis) and the standardised magnitude (vertical axis) of an AMS event.

Both types of spatial coherence are of importance. Event-type coherence is important for large-scale event response planning, such as provision of disaster management capacities for widespread floods. For the (re-)insurance industry that partly operates on an annual basis, non-event-type coherence is important as well because flood losses will cumulate throughout the year. Non-coherent years or periods are not interesting in the context of this paper. In such periods, AMS values occur randomly, and there is no signal that could be used for informing large-scale risk management or (re-)insurance.

There is little systematic work on spatial coherence of river flooding. Several studies have looked at spatial coherence of flood occurrence or magnitude (for an overview see Hall et al., 2014) but, to the authors' knowledge, no study has attempted to quantify the degree and type of coherence. Most studies have qualitatively compared flood activity for different catchments, for example, by averaging the number of flood events over a certain period, often 30 years, and comparing whether periods of increased flood occurrence are synchronized in different catchments. In contrast, Merz and Blöschl (2003) define spatial coherence as the spread of catchments which have their AMS value of a hydrological year on the same day. Hence, their quantitative analysis is limited to event-type coherence.

In this study, the spatial coherence of river flooding across Germany is studied by analysing fluctuations in AMS values at 68 discharge gauges for the common time period 1932-2005. Spatial coherence of flooding within each hydrological year and the type of coherence (or non-coherence) is quantified. An attempt is made to understand the processes which lead to spatial coherence by analysing the role of catchment wetness and event precipitation. This study builds on a recent paper (Merz et al., 2016), which used the same streamflow data set. Merz et al. (2016) characterized the temporal clustering of floods in Germany for different time windows and for different thresholds for partial duration series, but coherence in space was not analysed.

Chapter 2 introduces the study area and describes the data. In chapter 3, the indicators describing the flood characteristics, the initial catchment state and the event precipitation are introduced, and the methods to quantify spatial coherence and the underlying drivers are given. Results are presented in chapter 4, followed by the discussion and conclusions.

2. Study area and data

2.1 Study area and selection of catchments

Germany is characterised by a gradient of increasing continental climate from west to east and a gradient of increasing elevation from north to south. Both gradients lead to clear patterns of precipitation, temperature and snow coverage with implications for streamflow regimes and flood generation. For example, the mean annual snow cover duration follows a north-west south-east gradient with less than 20 days with snow cover to 80 days and even to more than 200 days in the south-eastern rim of Germany (BfG, 2003). Moisture fluxes into the target region are due to prevailing westerly winds and high intensity precipitation events are usually associated with cyclonic weather patterns. The advection of warm and moist air masses from the Mediterranean, referred as Vb pattern, occasionally leads to intense precipitation events and severe flooding over south and east Germany.

68 stations have been selected with mean daily discharge data for the common period 1932-2005. Although the mean daily flow may underestimate flood peaks in smaller catchments, this effect does not influence the overall results, since standardized AMS values (with zero mean and variance of one) are used. Fig. 3 shows the selected gauges. Table S1 (in supplement) lists the associated catchments and their main characteristics. The set of gauges and the time period is the same as in Merz et al. (2016). This selection was based on the following considerations. Firstly, the gauges are distributed all over Germany to cover the different flood generation settings. Further, a large number of gauges was sought for a common time period which should be as long as possible. Catchments smaller than 100 km^2 were excluded based on the assumptions that land use changes and flood retention basins play a more significant role in smaller catchments, and thus may disturb the signal.

Catchments with significant data gaps were excluded. Details about the station selection and the data set are given in Merz et al. (2016).

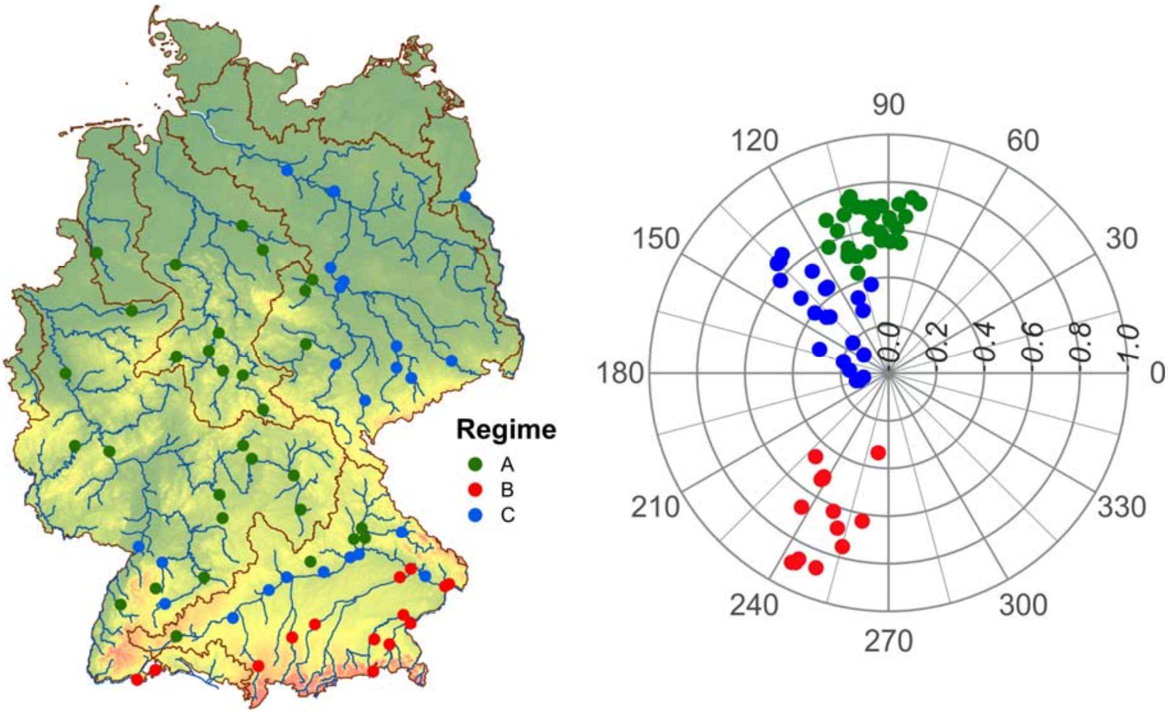

Fig. 3: Left: Study area and locations of river gauges including their flood regime. Right: Flood seasonality of the 68 gauges showing the mean timing of the AMS and the variability of the AMS timing for each gauge. The mean timing is expressed by the angular position starting from 1 for the first day of the hydrological year (1st November). The variability in flood timing is expressed by the radius value. A variability measure close to 0, i.e. in the centre of the polar plot, indicates large heterogeneity in flood timing. A variability measure close to one indicates that AMS events tend to occur around the same day in the hydrological year.

The 68 gauges are grouped into three regions based on their flood seasonality. Annual peak flow (AMS) values and the corresponding occurrence dates were extracted from the 74-year daily runoff at each station. Using directional statistics (Burn et al., 1997), two measures of flood seasonality were computed for each station: (1) the mean direction MD, representing the average time of occurrence of AMS events; (2) the variability measure r, quantifying the variability of AMS occurrence about the mean date. A cluster analysis on MD and r was then performed using the non-hierarchical K-means method. It should be noted that AMS values themselves were not used in the clustering analysis.

Fig. 3 shows the resulting three clusters. Region A consists of 31 stations and stretches across the western and central part of Germany from the north to the Danube River in the south. Floods occur predominantly in winter, typically triggered by westerly atmospheric flows resulting in prolonged precipitation phases in combination with wet catchments. The mean timing of AMS events varies from 80 to 119 (day-of-the-hydrological-year), i.e. from end of January to end of February. Region B is rather limited and contains 14 stations in south Germany. These are the southern tributaries of the Danube with summer floods. The mean date of AMS floods varies from middle of June to end of July. Floods are triggered by heavy precipitation events in the mountainous areas and/or by snowmelt events. Region C with 23 gauges covers the eastern part of the study area and a west-east stretch in the south of Germany including the Danube River. Floods occur mainly in winter, however, spring and summer floods do also occur. The measure of variability in flood timing indicates that the timing of AMS floods is very variable for some gauges of region C.

Our clustering result is very similar to that of Beurton and Thieken (2009) which is based on the monthly distribution of AMS values at 481 streamflow gauges throughout Germany. The difference between the two clustering analyses is that their groups of homogeneous stations are more patchy, i.e. adjacent stations tend to be more often in different flood groups. Our grouping is also in line with Mediero et al. (2015) who used fewer, but longer flow time series in Europe. They highlight the positioning of Germany at the intersection of three large-scale European regions, namely the Atlantic, Alpine and Continental regions which correspond to our regions A, B and C, respectively.

2.2 Data

The flood data set consists of mean daily flow records provided by different water authorities in Germany. They are part of the official hydrometric network and the stations and observations are regularly checked and can be assumed to be reliable. We used daily gridded (6x6 km) precipitation derived from more than 1440 stations of the German Weather Service covering (starting 1901) the analysed time period. The stations are rather homogeneously distributed across Germany. The data were homogenized and quality checked at Potsdam Institute for Climate Impact Research, according to Österle (2001) and Österle et al. (2006), correcting non-natural inhomogeneities such as changes in the station location, measurement methods or devices. Gaps of a station time series were filled by finding the neighbouring station with the highest correlation and adding the relative difference between the long-term monthly mean values of both stations to the neighbouring station's value.

3. Methods

We derive a set of indicators representing different characteristics of the AMS floods for the 68 selected catchments. Our indicator set includes, in addition to the magnitude and timing of AMS values, proxies for the catchment wetness (CW) and for event precipitation (EP) averaged across the catchment. CW represents the state of the catchment at the start of an AMS event and is therefore a proxy for the history prior to the AMS start date. EP considers the period between the flood event start date and AMS date, i.e. the event-built-up period (Nied et al., 2014). In this way, we attempt to separate the effects of initial catchment conditions from those of the event precipitation.

For each indicator, we use annual time series for the hydrological year (1 Nov. – 31 Oct.) and seasonal time series (winter: 1 Nov. – 30 Apr.; summer: 1 May – 31 Oct.). For better comparability and use in the statistical analyses, the indicator time series are standardized to zero mean and unit variance. Since we are interested in the correlation in flood characteristics, all indicator time series are detrended prior to the analysis. If two time series have a common temporal trend, this could inflate their correlation.

3.1 Indicators for flood characteristics

For each of the 68 catchments, three AMS (annual, winter, summer) time series are derived, whereas an AMS event has to be a peak, and two neighboring AMS events have to be at least seven days far from each other. These criteria could be important if an AMS value occurs at the start or the end of a hydrological year. Otherwise it is likely that two values belonging to the same event are counted twice. In such cases the second largest peak in the hydrological year was selected.

We need an indicator to quantify the event-type strength of a certain hydrological year, which indicates whether the AMS values across Germany are clustered in a few events (event-type) or are distributed throughout the year (non-event-type). We tested the measure of the variability of flood occurrences r, however, this measure cannot well distinguish between situations where AMS are distributed throughout the year and where the AMS are clustered in a few events and the timing of these events is opposite to each other in the directional space.

We propose an alternative indicator of event-type strength based on the following considerations: (1) AMS values of different gauges are defined to belong to one flood event when they occur within a time window of at most 14 days. This period considers that atmospheric circulation patterns persist for a few days with a median persistence from three to five days (Petrow et al., 2009). It further takes into account the travel time of flood waves within the river network. 14 days is the maximum time period that we consider reasonable for the flood event built-up period in Germany. (2) To single out flood events for a given hydrological year, we select the time window (of at most 14 days) which contains the highest number of AMS values across Germany. This step is repeated with the remaining AMS values until all AMS values are assigned to flood events. This results for each hydrological year in *n* non-overlapping flood events, each containing at least one AMS value. (3) These *n* flood events are transferred into an indicator which considers the number of AMS values within a flood event. For example, suppose that there are two years with several flood events in each year (Fig. 4). In year A, 95% of the gauges are contained in one event, whereas in year B one third of the AMS values are assigned to each event. We thus regard year A as more of event-type compared to year B. We derive the cumulative distribution of the number of flood events, whereas the ordinate expresses the fraction of catchments contained in each event, when the events are ordered according to the number of AMS values. We define the event-type indicator as the area above the cumulative distribution function (Fig. 4). The smaller the area, the more inclined the year is towards event-type flooding.

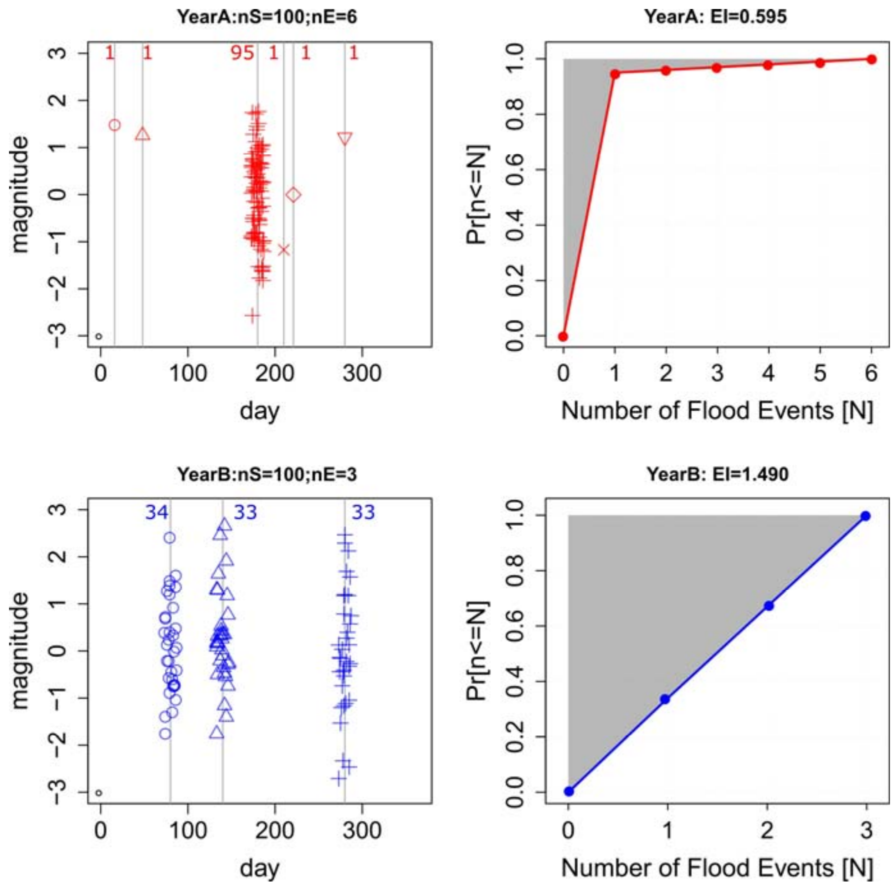

Fig. 4: Schematic to explain how the event-type indicator EI is quantified. Left panel: Distribution of flood events throughout the hydrological year. Numbers next to the vertical lines (indicating an event) give the number of gauges contained in that event. Right panel: EI is computed as the shaded area bounded by the distribution curve.

3.2 Catchment wetness indicator

We use the streamflow value prior to each AMS event as proxy for catchment wetness. Pre-event streamflow is a widely used proxy for the initial catchment state (e.g. Ettrick et al., 1987, Plate et al., 1988). It is easily derived from runoff time series and does not require additional data unlike other proxies, such as antecedent precipitation or soil moisture. Pre-event streamflow was found to significantly correlate with runoff coefficients in humid catchments (Longobardi et al., 2003). It correlated similarly well to runoff coefficients as pre-event soil moisture. The antecedent precipitation index was found inferior to pre-event streamflow to characterize runoff generation (Longobardi et al., 2003).

For each AMS value at each gauge the start day of the flood event is identified. We apply a modified gradient-based method suggested by Klein (2009), which is an empirical method of identifying a starting point of the rising hydrograph limb providing some constraints on the gradient changes between daily flow values. Furthermore, constraints are imposed to distinguish between dependent (e.g. double-peak hydrographs) and independent flood events. The empirical thresholds are selected and tested for all 68 gauges to yield a robust separation, as one would do manually based on the visual hydrograph inspection. A similar approach was taken by Merz and Blöschl (2009) to identify the start points of direct flow hydrographs.

In the first step, an independent flood event preceding each AMS flood is identified by combing the criteria after Bacchi et al. (1992) and LAWA (1997). This is needed to avoid small hydrograph spikes being treated as flood events independent from the AMS flood. A local maximum is regarded as a local flow peak if it is higher than 20% of the AMS flow and the local minimum between peaks drops below 70% of the lower peak. The AMS peak and the preceding lower peak are considered to be independent if either the time span between both (DT) exceeds a threshold value or the local minimum drops below 20% of the AMS value. We found DT=10 days as efficient to separate individual peaks.

In the second step, the gradient in daily flows is computed between consecutive days. A gradient threshold is selected as the 10% percentile of the empirical distribution. A pre-event flow is detected as the minimum flow in a DT-period of consecutive days with the gradient below the selected threshold. This window characterizes a period of stable flow conditions and can be regarded as characteristic for the catchment state. In case no period of length DT is identified between independent flood peaks, the minimum flow between the two is taken as an indicator for antecedent catchment wetness. Empirical thresholds are selected in an iterative procedure by visually inspecting the results of hydrograph separation at all gauges. The detected flood start date corresponds well to visual detection of the start of the rising hydrograph limbs.

3.3 Event precipitation indicator

We use the precipitation amount during the built-up period as indicator of the event meteorology. For the 68 catchments, the daily precipitation is averaged over the catchment area. There are some catchments whose headwater sub-catchments are located outside of Germany. Since precipitation data are only available for Germany and the sub-catchments in Austria and the Czech Republic, the average precipitation outside this domain is assumed to correspond to the catchment precipitation in the data-covered domain. Out of 68 catchments 48 catchments are covered by precipitation data by more than 90%. In the 20 remaining catchments only very few have a coverage of less than 50%. Due to averaging the precipitation over the entire catchment to build the precipitation indicator, we do not expect that our assumption of homogeneous precipitation has a large impact on the results. However, it is certainly a limitation of the study and can only be resolved over time, when more comprehensive long-term precipitation datasets become available. Unfortunately, no daily resolved precipitation dataset for Central Europe exists dating back to 1932. The recently released ERA-20C reanalysis dataset is not suitable because it does not reproduce daily precipitation events. Since only wind fields are assimilated into the climate models, only the monthly climatology in ERA-20C can be considered reliable (Poli et al., 2016).

For each AMS value, daily catchment precipitation in the event built-up period, defined as the period from the date of the detected pre-event flow to the AMS date, is analysed. If the pre-event flow is dated back more than 14 days from the AMS, a maximum time window of

15 days (including the AMS date) is taken for the analysis. Ideally, one would select the time window corresponding to the catchment concentration time to assess the flood event precipitation. This is, however, difficult; empirical estimates of concentration times may differ up to 500% between different methods (Grimaldi et al., 2012) and depend not only on the catchment characteristics but also on the event magnitude. The event precipitation is computed as the precipitation sum of all days prior to the AMS date including the precipitation peak till the first dry day within the selected time window. A day is considered dry, if the catchment precipitation drops below 1 mm/d. The threshold is taken to avoid spurious precipitation, which is not relevant for runoff. Due to averaging of precipitation over large catchment domains some small precipitation amounts can emerge thus enlarging the pre-event precipitation duration, but the amount is too small to cause notable flow changes.

We tested both the catchment precipitation amount and precipitation intensity during the built-up period as indicator for event precipitation. The results were very similar, and thus the amount is used in the following.

3.4 Standardized anomaly index

To increase the signal-to-noise ratio, composite time series are compiled for the different indicators. The idea is that these composite time series represent the large-scale behaviour, whereas the at-site time series may be contaminated by local influences. Composite time series may be helpful in distinguishing the underlying large-scale signal at a site from local noise and local effects. Large-scale or national composites have often been used, e.g. Robson et al. (2002), McCabe and Wolock (2002), Kiem et al. (2003), Lindström and Bergström (2004), Petrow et al. (2009).

We use the standardized anomaly index (SAI) defined as the average of the standardized station time series x_{ij} over the M stations, where i=1,…,N denotes the year, j=1,…,M denotes the station (Katz and Glantz, 1986):

$$SAI_i = \frac{1}{M} \sum\nolimits_{j=1}^{M} x_{ij}$$

The stations were given equal weight, since we focus on the temporal variations, rather than on the true average (Lindström and Bergström, 2004). Composites are determined for the entire data set of 68 gauges and, additionally, for the three flood regime regions.

3.5 Degree of spatial coherence

The strength of spatial coherence is quantified using the external variance ratio EVR (Katz and Glantz, 1986, Moron et al., 2006):

$$EVR = \frac{\sigma_{EXT}^2}{\sigma_{EXT}^2 + \sigma_{INT}^2}$$

EVR is defined using the external variance σ_{EXT}^2 that is common to all stations and the internal variance σ_{INT}^2 that is associated with differences between stations:

$$\sigma_{EXT}^2 = var(SAI) - \left(\frac{1}{M}\,\sigma_{INT}^2\right)$$

$$\sigma_{INT}^2 = \frac{1}{N\,(M-1)} \sum_{j=1}^{M} \sum_{i=1}^{N} \left(x_{ij} - SAI_i\right)^2$$

The interannual variance of SAI is given as:

$$var(SAI) = \tfrac{1}{M} + \left(1 - \tfrac{1}{M}\right)\,\bar{\rho}$$

where $\bar{\rho}$ is the mean interstation correlation. If all stations are independent, then $var(SAI) = {}^{1}/_{M}$. If all stations are perfectly correlated, $var(SAI) = 1$ (Katz and Glantz, 1986).

3.6 Multiple linear regression and relative contributions

AMS coherence within a hydrological year (or for an even more prolonged period) can be caused by event precipitation and/or catchment wetness consistently above or below average throughout the considered period. To understand to which extent either of these two factors contribute to spatial coherence of floods in Germany, the AMS composite is related to the composites of catchment wetness and event precipitation via multiple linear regression. Regression models are established for the composite of the entire station set and for the three regions corresponding to different flood regimes. Regression models are developed for the annual and seasonal series. At the 5% significance level, it is tested whether the coefficients of the multiple linear regression are significantly different from zero and whether interaction effects between the predictors CW and EP play a role.

To estimate the relative importance of the predictors, i.e. the proportion of the variance explained by the individual predictors, the relative partial sum of squares (RPSS) (Gardner and Trabalka, 1985) is used. $RPSS_k$ for predictor k is calculated by dividing the difference between the residual sum of squares (RSS) for the model without predictor k (RSS_{-k}) and for the full model by the total sum of squares (TSS):

$$\mathrm{RPSS_k}\ [\%] = 100 * (\mathrm{RSS_{-k}} - \mathrm{RSS})/\mathrm{TSS}$$

4. Results

4.1 Degree of spatial coherence

Fig. 5 visualizes the spatial coherence of flood characteristics across the 68 gauges for the period 1932-2005. The top two panels show the number of flood events and the standardized AMS magnitude for each hydrological year. The number of flood events is derived by extracting peak-over-threshold values (POT) with on average one peak per year. The extraction is based on the USWRC (1976) procedure as described in Lang et al. (1999).

Both flood indicators (number of floods and standardized AMS magnitude) show a clear spatial coherence, although the effect is stronger for the number of floods. Single years tend to have the same colour across many (or even all) gauges. The vertical patterns extend often across the three flood regions. This is remarkable as region B has a distinct summer flood seasonality whereas the floods in regions A and C occur typically in winter. From this plot we can conclude that there is a tendency for spatial coherence in flooding even across flood regime regions. We also see that these patterns have a short persistence, at most a few years.

Fig. 5 also shows CW and EP, i.e. the standardized streamflow at the start day of each AMS event and the standardized event precipitation amount, respectively. There are some vertical stripes illustrating that catchment wetness and/or event precipitation have been consistently above or below average for many stations across Germany in some years. However, the space-time patterns of CW and EP are noisier indicating a lower degree of spatial coherence compared to the AMS values or number of floods.

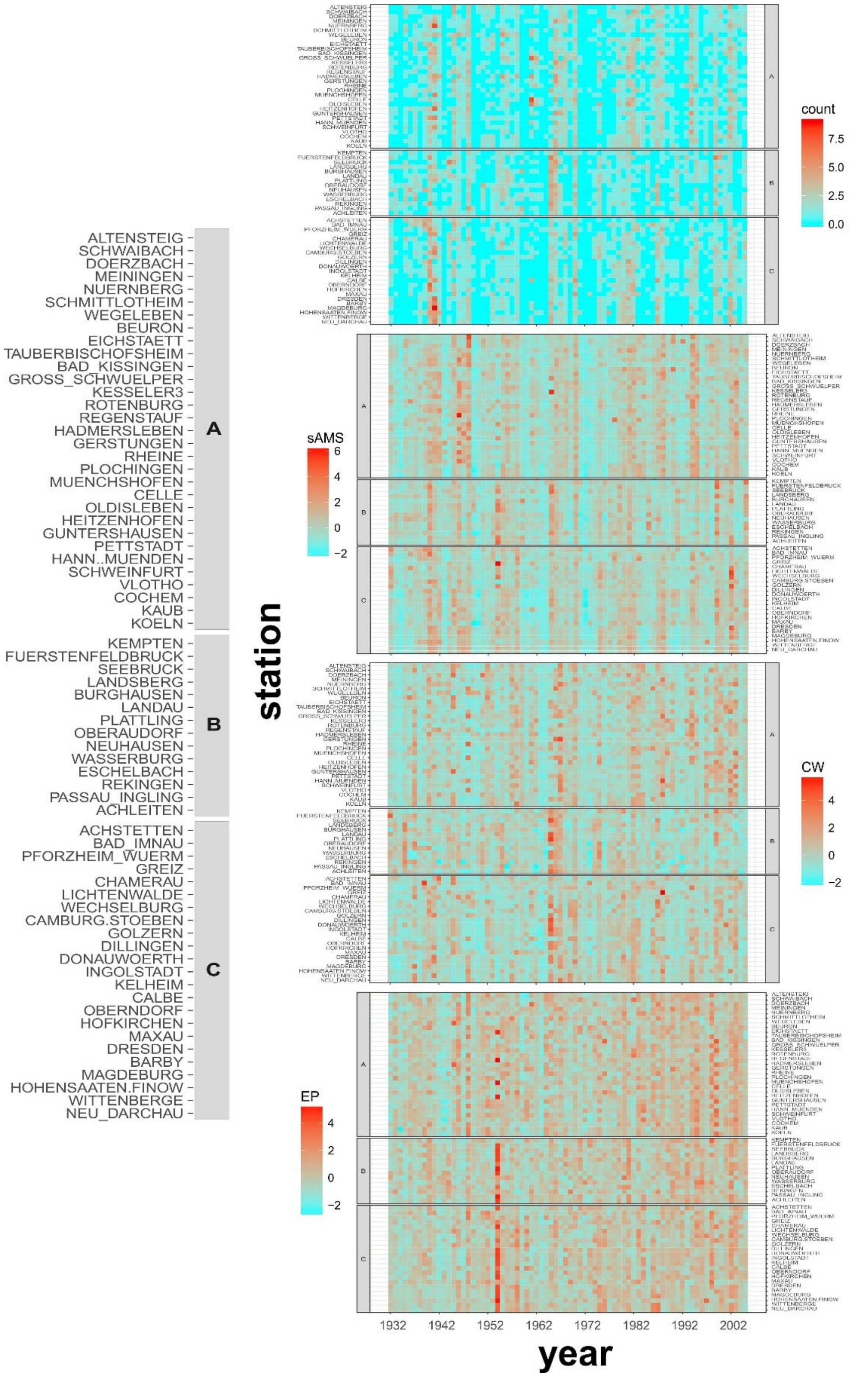

Fig. 5: Space-time patterns of flood characteristics. From top to bottom: Number of POT1 events per hydrological year, standardized AMS, standardized CW and standardized EP across 68 catchments for 1932-2005. Catchments are grouped according to flood regimes and catchment area (catchment size increase from top to bottom within each region).

Table 1 shows the external variance ratio EVR for AMS, CW and EP for the entire set of catchments and for the three regions. EVR values are given for the annual and seasonal series. Table 1 indicates significant coherence for AMS values. For instance, EVR = 38% for the annual series and the complete set of gauges, i.e. 38% of the variance in AMS is common to all gauges. These values are much higher for the regions, for example, EVR reaches 57% for region B. The increase in EVR for the regions is expected as these stations have a similar flood seasonality and tend to be closer together. In the winter season, EVR values tend to be higher than in summer. For instance, almost half of the variance is common to all gauges for AMS. This is a consistent result for all three indicators and the complete set of gauges: The spatial coherence tends to be stronger in the winter season compared to the summer and annual series.

Table 1: Annual and seasonal spatial coherence measure EVR [%] for the flood, catchment wetness and event precipitation indicators for the complete set of catchments (ALL, 68 stations) and the three flood regime regions (A: 31 stations; B: 14 stations; C: 23 stations).

	AMS				CW				EP			
Region	**ALL**	**A**	**B**	**C**	**ALL**	**A**	**B**	**C**	**ALL**	**A**	**B**	**C**
Annual	37.6	49.2	57.0	48.5	23.7	30.8	36.6	30.1	23.3	29.4	38.7	39.6
Winter	47.3	57.3	56.2	53.6	30.8	35.0	37.6	35.6	25.8	36.5	40.5	31.4
Summer	33.6	42.0	60.5	44.4	24.0	28.3	38.5	31.2	25.5	31.7	42.4	35.7

EVR is clearly larger for AMS (38% for annual values) compared to EVR for CW (24%) and EP (23%). Hence, the common signal across the 68 gauges is quite strong for AMS, but lower for CW and EP. The same is true for the two seasons.

There may be several factors explaining higher EVR for AMS compared to CW and EP. First, it is likely that there is a combined effect of both factors on AMS and not only one of those is dominant. Second, the river network effect, which is not explicitly considered in our analysis, may contribute to higher EVR of AMS, since a number of nested catchments are present in the dataset. However, this effect also affects the CW indicator which is based on the pre-event flow. Further, our CW and EP indicators are rather simplified proxies and cannot describe the system conditions perfectly.

Comparing the EVR values between the three regions shows that region B tends to be the most coherent in terms of AMS, CW and EP. The difference in EVR values between region B and regions A and C is particularly large for AMS in summer (61% for B; 42% and 44% for A and C, respectively). Floods in region B can be caused by different processes, in particular heavy precipitation events in the mountains, some of them of convective type, and events with a snowmelt contribution. Hence, the larger coherence of region B cannot be explained by a certain flood generation mechanism which is more spatially homogeneous. It is rather a consequence of the much smaller geographical extent of region B (roughly 60,000 km^2) compared to A (180,000 km^2) and C (120,000 km^2).

These results show significant spatial coherence in AMS values and number of flood events, despite different flood regimes and a large spatial extent of Germany. Stratification in flood regime regions increases the spatial coherence indicator EVR. However, in most cases the increase in spatial coherence is modest. This suggests that floods (and CW, EP) are related to some large-scale variability which acts beyond the effect of single precipitation events and flood regimes. Stratification in winter and summer does not change EVR values in a consistent way. In many cases EVR values increase, as one would expect due to the smaller time period when looking at seasons, but in some cases the spatial coherence seems to decrease. The latter cases occur typically for the comparison between annual and summer series. This might be explained by the flood seasonality and differences in flood generation. For example, EVR decreases from 49% to 42% for AMS in region A.

Because region A has a distinct winter flood regime, and winter floods in Germany tend to have a larger spatial extent compared to summer floods (Uhlemann et al., 2010).

4.2 Understanding the type of spatial flood coherence

To give an impression of the different situations that can be found in the data set, Fig. 6 shows the timing and magnitude of three selected hydrological years. The complete set of years is given in Figure S1 (supplement).

The year 1941 represents a non-event-type, coherent year. It is the year with the highest value of the event-type indicator *EI* within the period 1932-2005. The AMS values are spread out through the year. AMS magnitudes are in a similar range, i.e. the magnitude of summer floods in regions B are not far from winter and spring floods in regions A and C. 1952 represents an event-type, coherent situation. The 68 AMS values are again within a rather narrow magnitude range, but now they are clustered in only six events. Again, coherence extends beyond flood regimes. Finally, the year 1954 represents an event-type, non-coherent year. The AMS values are clustered in six events, but the AMS magnitudes are spread across a wide range. It is the year with the highest variability in AMS magnitude, i.e. the most non-coherent year. Non-coherence is caused by the large spread in magnitude of one summer event affecting gauges from all three flood regimes.

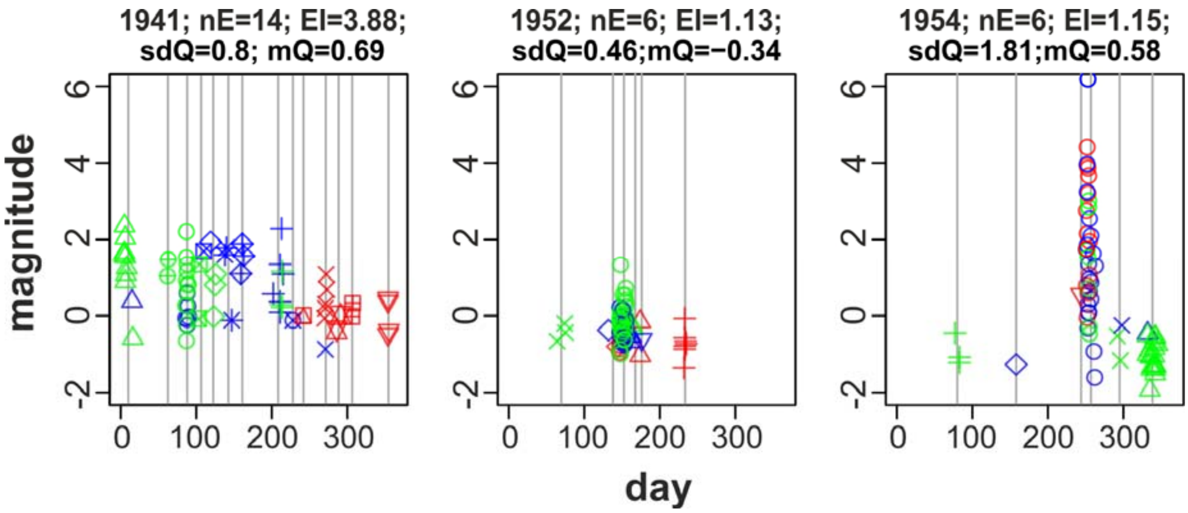

Fig 6: AMS values for the 68 catchments for selected hydrological years. The horizontal axis shows the day of the year, the vertical axis the standardized AMS magnitude. Vertical lines indicate an event with at least one AMS occurrence. Different colors indicate the flood regimes (Green: Region A; Red: Region B; Blue: Region C). Different symbols indicate different events. Abbreviations: *n*: number of flood events; *EI*: event-type indicator; *sdQ*: indicator of magnitude coherence, i.e. standard deviation of 68 AMS magnitudes (standardized); *mQ*: mean of 68 AMS magnitudes (standardized).

Figure 7 shows the relation between the event-type indicator, the magnitude coherence and the average AMS magnitude for all 74 hydrological years in the period 1932-2005. Large values along the vertical axis signify non-event-type years where AMS values occur throughout the year. The horizontal axis represents the degree of coherence in AMS magnitude. It is quantified by the standard deviation of the AMS values for a certain hydrological year. The size of two digit years in the plot is proportional to the mean value of the 68 AMS magnitudes, with above-average years coloured in red.

Interestingly, the upper right corner of Fig. 7 is blank, i.e, the data set of 74 years does not contain years where both the AMS magnitude and AMS timing are spread across a wide range. The lower right corner (event-type / non-coherence) shows above-average years where AMS values tend to cluster in time. The spread in AMS values is often caused by a single event affecting a considerable number of gauges, but with different AMS magnitudes. Most of the years can be assigned to the lower left corner (event-type / coherence). The AMS values at the 68 gauges cluster in a few events, and these AMS values are within a rather limited range. Finally, some years are located in the upper left corner (non-event-type / coherence).

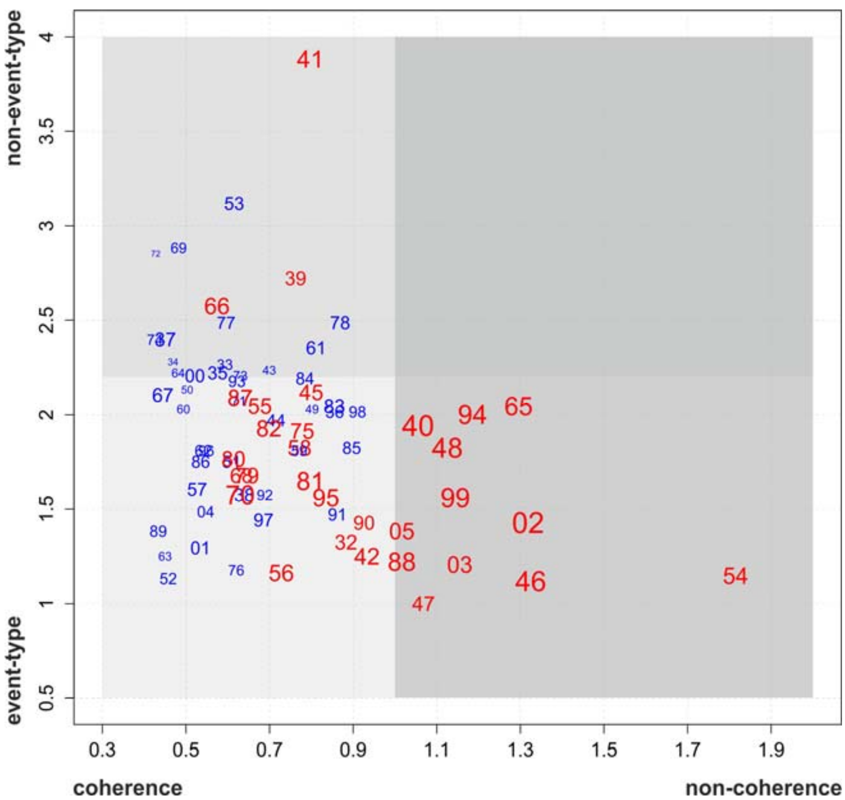

Fig 7: Spatial coherence versus event-type indicator for all hydrological years 1932-2005. Each year is marked by the last two digits. The size of the digits represents the average AMS magnitude. Above-average flood years are marked in red, below-average flood years in blue.

From Fig. 7 we can conclude that considerable spatial coherence of AMS values exists. Many years are located in the left part of the diagram. Spatial coherence can be found in event-type and non-event-type years. The fact that many years, where the AMS timing is rather spread throughout the year, are coherent, suggests that German catchments often tend to be in a wet or dry state when there is some similarity in AMS magnitude across flood regime regions.

There is a slight tendency to stratify in above-average, non-coherent years and below-average, coherent years. This means that AMS magnitudes tend to be similar throughout the year for years without extreme floods. For high flood years, AMS values vary much more.

4.3 Role of event precipitation and catchment wetness

To answer the question whether the variability in AMS is predominantly linked to the catchment wetness or event precipitation, multiple linear regression models are established, whereas the composites for CW and EP are used as predictors for the AMS composite. Fig. 8 visualizes the relative importance of CW and EP in explaining AMS variability and the variance explained by the multiple linear models. Twelve models are developed for the different time scales and regions. It should be noted that in all cases both CW and EP are significant predictors at the 5% level, whereas the interaction term between CW and EP does not play a significant role.

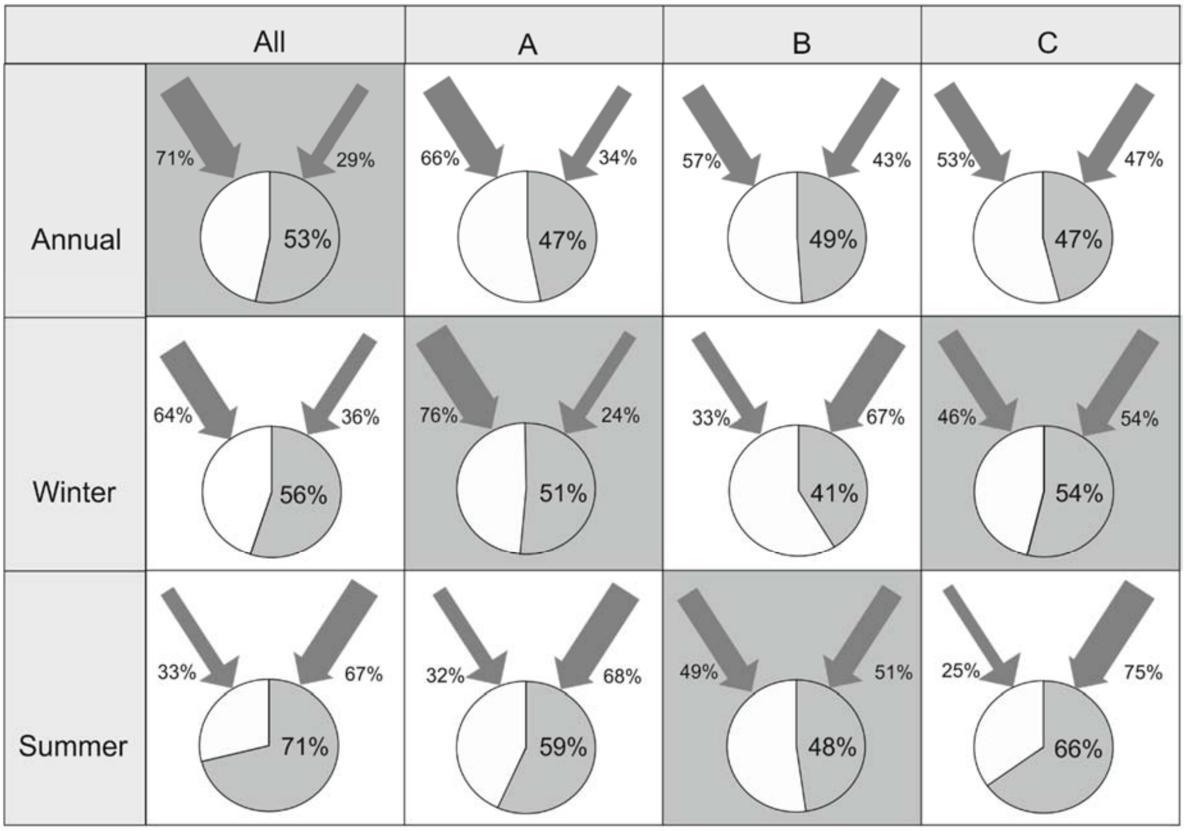

Fig 8: Relative importance of catchment wetness CW (left arrow) and event precipitation EP (right arrow) in explaining AMS variability for the complete set of gauges and the flood regime regions (columns) and for annual and seasonal series (rows). The thickness of the arrows indicates the relative importance. The explained variance is indicated as dark shaded segment of the pie chart. The light grey boxes show the more important cases, i.e. the dominant flood season for the different regions and the annual values for the entire station set.

For the annual series and the entire set of gauges, 53% of the AMS variability is explained by the CW and EP composites. It is interesting that the region-specific models are not able to obtain a higher share of explained variance than the models for the entire data set. The stratification in seasons improves the model skill for the entire set and the regions A and C. Possibly, seasonal AMS have smaller variability and are thus better explained by the selected predictors.

For the entire set of gauges, CW dominates the model with a relative importance of 71%. For the regions this dominance of CW is less pronounced. Comparing the relative contributions of CW and EP for the seasons, there is a tendency for CW being more important in winter and EP gaining importance in summer. This effect is in line with the variability of CW and EP. CW shows a larger variability than EP in winter, and the variability of EP increases for summer. This result agrees with the major flood generation processes. For instance, summer floods are more often caused by convective events linked to higher variability in event precipitation.

The highlighted boxes in Fig. 8 show the more important cases, i.e. the dominant flood season for the different regions and the annual values for the entire station set. Region A and C are winter-dominated. CW plays a dominant role in region A with a contribution of 76%. Floods occur typically as consequence of long-lasting, but not very intense precipitation events on wet catchments. Hence, the initial conditions play an important role. For region B and C, EP and CW have a similar contribution. These regions are either summer-dominated (region B) or winter-dominated but with the possibility of large summer floods caused by very intense rainfall (region C). This explains the comparatively larger role of EP for regions B and C.

The analysis finds a tendency that higher floods in the current season are linked to higher floods in the season ahead. This effect can be caused by persistence of EP across seasons or by persistence in CW. Fig. 9 visualizes the Spearman correlation coefficients for the three indicators within and between the seasons. EP is not significantly correlated between the seasons. Hence, the significant correlation of seasonal AMS composites is related to CW. For the entire data set, a wetter winter half-year (higher CW and AMS) leads to higher CW in the following summer, and consequently to higher summer AMS. This effect works similarly, but somewhat weaker, for the transfer from summer to winter.

Overall, the regions show a similar behavior compared to the entire data set. The most striking difference is the zero correlation between the AMS values in summer and the following winter in region B: High summer floods do not lead to higher winter floods. This is expected as floods in this region are either related to snow melt or caused by convective summer rainfalls. In both cases, this does not lead to a strong increase in CW because the water tends to leave the catchment more rapidly, e.g. via a larger share of overland flow. Moreover, we can assume that higher slopes and shallower soils in these steep mountain catchments in southern Germany contribute to this effect as well.

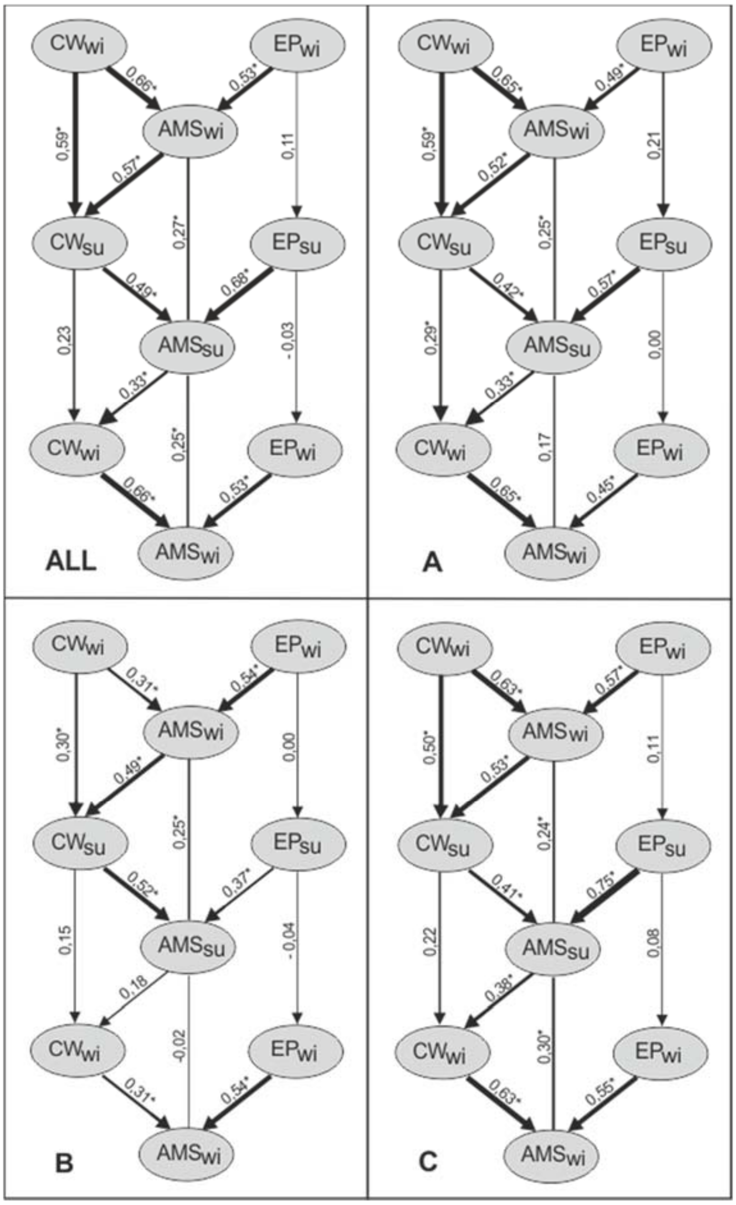

Fig 9: Intra-season and inter-season Spearman correlation coefficients AMS, CW and EP for the entire station set and the three regions. The thickness of the arrows is proportional to the correlation coefficient. Stars indicate statistical significance at 5%.

5. Discussion

Recently, the occurrence of flood-rich and flood-poor periods has found increasing interest in the scientific literature on flood changes (Hall et al., 2014). However, the societally important question whether such periods are in phase across regions has not be studied in a systematic way. We propose several indicators to quantify and understand the spatial coherence of flood activity. One of them, the event-type indicator *EI*, is proposed to assess whether the annual maxima in a given hydrological year within the study region occur in one or a few events or are distributed throughout the year. Although we propose this indicator for AMS values on an annual basis, other time periods and other flood characteristics, e.g. POT values, could be used.

The application of these indicators to Germany finds that flood-rich and flood-poor periods tend to be in phase, suggesting a substantial spatial coherence in flood activity across the three flood regime regions. These flood-rich and flood-poor periods have a short persistence of at most a few years, and are not visible on the decadal time scale. This was also found and discussed in detail by Merz et al. (2016).

In most of the years of the study period, the flood activity can be described as coherent and of event-type, i.e. the AMS values of the different catchments tend to occur in a few events and in similar magnitude range. There are also a number of years where the AMS timing is spread throughout the year (non-event-type), although the AMS magnitudes are similar. Both types of years suggest that annual maximum floods, and their drivers catchment wetness and event precipitation, are conditioned on some large-scale variability beyond flood regime regions and single flood events.

Non-coherent years are typically of event-type and have above-average magnitudes. This is the consequence of one or a few large events which affect many catchments but with varying magnitudes. Hydrological years with extreme floods tend to be non-coherent. This result is sensible from a climatological point of view. Extreme floods are often of smaller spatial scale, such as the Vb weather pattern caused floods mentioned in the introduction. A prominent example is the year 2002 with disastrous flooding in the Elbe and Danube catchments.

The analysis of the underlying drivers of spatial coherence of flood activity reveals the relative role of catchment wetness and event precipitation. Although their importance varies between the regions and seasons, as function of the different flood generation mechanisms, catchment wetness tends to dominate. The significant correlation between the AMS composites in subsequent seasons is a consequence of persistence in catchment wetness across seasons and not by persistence in event precipitation. The weaker correlation between summer and subsequent winter could be caused by the larger role of evapotranspiration in summer. Evapotranspiration depletes the soil moisture storage thus cutting the transfer link. High CW and AMS values during summer might be more easily overwritten by evapotranspiration.

Finally, we note that our study has a numbers of limitations. The analysis builds on observed streamflow and precipitation data which include gaps that were filled using correlation analysis. These time series are part of the official station network of the German Weather Service and a number of water resources authorities, and are expected to be well maintained and quality checked. Time series with large gaps were not included in the analysis. Some of the catchments have areas outside of Germany for which no high-quality data are available to us. We believe that our assumption to fill these gaps is the most reasonable one, and that it does not impact our findings.

Further, the proposed method and analysis include a few choices and subjective thresholds. We have tried to substantiate these choices and thresholds in all cases, and wherever feasible, assess the sensitivity of the results to these choices. For example, the assumed time window of 14 days in the definition of flood events is based on physical considerations, such as the travel times of flood waves in the river network. Further, it has been tested that the variation of this value does not substantially influence the results – in this case the distribution of hydrological years in the event-type – coherence space (as in Figure 7; results of the test are not shown). Although the exact numerical results of our empirical study would vary when using different data sets and different threshold values, we are convinced that the overall findings would not be impacted.

A final note of caution is related to possible temporal changes in our time series. Our indicator time series have been detrended prior to the analysis. In addition to the arguments for detrending presented in chapter 3, we report here that the composite flood time series do not show significant changes for the complete set of gauges and for the three regions. Based on the Mann-Kendall test, the Null hypothesis of no trend cannot be rejected even at the 10% significance level. However, an interesting question arises in regard to the recent study of Blöschl et al. (2017) who found consistent patterns of changes in the timing of AMS events in Europe. If the flood timing changes within a region, this could affect the type of coherence. Figure 10 gives the times series of the event-type indicator *EI* and the coherence indicator *sdQ*. *EI* shows a significant downward trend (at 5%), whereas the change in *sdQ* is not significant. Hence, there is a tendency towards more event-type years, i.e. floods tend to spread out less during more recent years. The changes in flood timing in Germany can be roughly summarized by a tendency towards later floods in flood region A and towards earlier floods in region C (see Figure 1 in Blöschl et al., 2017). Hence, the two flood regimes A and C whose average flood timing is already rather close (Figure 3) seem to have moved closer to each other explaining the decrease in the *EI* value. This observation would deserve further analysis; an interesting question is whether this tendency could lead to a higher probability of large-scale floods with more catchments showing AMS events at the same time.

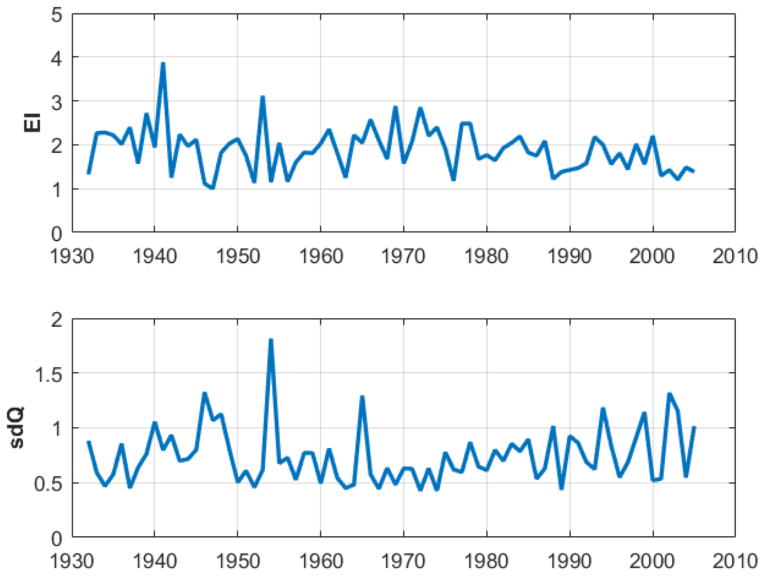

Fig 10: Time series of event-type indicator *EI* (top) and coherence indicator *sdQ* (bottom).

6. Conclusions

Despite its societal relevance, the question whether fluctuations in flood occurrence or magnitude are coherent in space has hardly been addressed. We investigate this question and find remarkable spatial coherence across Germany given its different flood regimes. There is a tendency that higher/lower-flood years in catchments, which are dominated by summer floods, coincide with higher/lower-flood years for winter flood-dominated catchments.

To better understand this phenomenon, we propose to differentiate in event-type and non-event-type coherence. Spatial coherence is seen for both types. There are quite a number of years with considerable non-event-type coherence, i.e. AMS values of the 68 gauges are spread throughout year but in the same magnitude range. Interestingly, high-flood years tend to be of event-type and non-coherent, i.e. there is often one event that affects many catchments with a range of magnitudes. This suggests that, although spatial coherence is a remarkable phenomenon, it plays a rather small role for years with larger ("interesting") flooding. Hence, we argue that spatial coherence in flooding has not been a severe problem for Germany. Large-scale flooding across Germany can lead to severe situations, however, extreme magnitudes across the country within one event or within one year seem to be rather unlikely.

We attempt to clarify the role of event precipitation and initial catchment state in shaping spatial coherence in flooding. Our findings indicate that coherence is caused rather by persistence in catchment wetness than by persistent periods of higher/lower event precipitation. Annual maximum floods and catchment wetness are conditioned on some large-scale variability beyond flood regime regions and single flood events.

The proposed indicators and the analysis build on observation data and include several assumptions and subjective choices. Although the specific numerical results would vary when using different data sets and data gap filling procedures, and when selecting different threshold values, we are convinced that the overall findings would not be impacted. An interesting observation is the trend in the event-type indicator, suggesting a tendency that, in recent years, a higher number of catchments have their AMS values at the same time. This observation can be explained by the detected shifts in flood timing across Germany and Europe by Blöschl et al. (2017). It deserves further study whether this tendency significantly changes the probability of large-scale floods in Germany.

Acknowledgements

We thank the Federal Agency for Cartography and Geodesy in Germany (BKG) for provision of the digital elevation model of Germany. We are grateful for providing the discharge data: Bavarian State Office of Environment (LfU), Baden-Württemberg Office of Environment, Measurements and Environmental Protection (LUBW), Brandenburg Office of Environment, Health and Consumer Protection (LUGV), Saxony State Office of Environment, Agriculture and Geology (SMUL), Saxony-Anhalt Office of Flood Protection and Water Management (LHW), Thüringen State Office of Environment and Geology (TLUG), Hessian Agency for the Environment and Geology (HLUG), Rhineland Palatinate Office of Environment, Water Management and the Factory Inspectorate (LUWG), Saarland Ministry for Environment and Consumer Protection (MUV), Office for Nature, Environment and Consumer Protection North Rhine-Westphalia (LANUV NRW), Lower Saxony Office for Water Management, Coast Protection and Nature Protection (NLWKN), Water and Shipping Management of the Fed. Rep. (WSV), prepared by the Federal Institute for Hydrology (BfG). We gratefully appreciate the provision of precipitation data by German Weather Service, kindly provided and processed by the Potsdam-Institute for Climate Impact Research (PIK).

References

Assani, A. A., Charron, S., Matteau, M., Mesfioui, M., Quessy, J.-F. (2010): Temporal variability modes of floods for catchments in the St. Lawrence watershed (Quebec, Canada). Journal of Hydrology 385: 292 - 299.

Bacchi, A., Brath, A., Kottegoda, N. T. (1992): Analysis of the relationships between flood peaks and flood volumes based on crossing properties of River Flo processes. Water Resources Research, 28(10), 2773-2782.

Beurton, S. and Thieken, A. (2009): Seasonality of floods in Germany, Hydrol. Sci. J., 54, 62–76, doi:10.1623/hysj.54.1.62.

BfG (2003): Hydrologischer Atlas von Deutschland (HAD). Bundeministerium für Umwelt, Naturschutz und Reaktorsicherheit (Ed.), ISBN: 3-00-005624-6

Blöschl, G., Hall, J., Parajka, J., Perdigão, R. A. P., Merz, B., Arheimer, B., Aronica, G. T., Bilibashi, A., Bonacci, O., Borga, M., Čanjevac, I., Castellarin, A., Chirico, G. B., Claps, P., Fiala, K., Frolova, N., Gorbachova, L., Gül, A., Hannaford, J., Harrigan, S., Kireeva, M., Kiss, A., Kjeldsen, T. R., Kohnová, S., Koskela, J. J., Ledvinka, O., Macdonald, N., Mavrova-Guirguinova, M., Mediero, L., Merz, R., Molnar, P., Montanari, A., Murphy, C., Osuch, M., Ovcharuk, V., Radevski, I., Rogger, M., Salinas, J. L., Sauquet, E., Šraj, M., Szolgay, J., Viglione, A., Volpi, E., Wilson, D., Zaimi, K., Živković, N. (2017): Changing climate shifts timing of European floods, Science, 357, 6351, 588–590, doi: 10.1126/science.aan2506

Böhm, O. and Wetzel, K.-F. (2006): Flood history of the Danube tributaries Lech and Isar in the Alpine foreland of Germany. Hydrol. Sci. J., 51:5, 784-798, doi: 10.1623/hysj.51.5.784

Burn, D. H. (1997): Catchment similarity for regional flood frequency analysis using seasonality measures. J. Hydrol., 202, 212-230

Ettrick, T. M., Mawdlsey, J. A., Metcalfe, A. V. (1987): The Influence of Antecedent Catchment Conditions on Seasonal Flood Risk. Water Resources Res., 23, 481-488.

Gardner, R. H., and Trabalka, J. R. (1985): Methods of uncertainty analysis for a global carbon dioxide model, Oak Ridge National Lab., TN (USA).

Glaser, R., Riemann, D., Schönbein, J., Barriendos, M., Brázdil, R., Bertolin, C., Camuffo, D., Deutsch, M., Dobrovolný, P., van Engelen, A., Enzi, S., Halíčková, M., Koenig, S. J., Kotyza, O., Limanówka, D., Macková, J., Sghedoni, M., Martin, B., Himmelsbach, I. (2010):

The variability of European floods since AD 1500. Climatic Change, 101, 235-256, doi: 10.1007/s10584-010-9816-7

Grimaldi, S. Petroselli, A. Tauro, F., Porfiri, M. (2012): Time of concentration: a paradox in modern hydrology, Hydrol. Sci. J. 57(2), 217-228.

Hall, J., Arheimer, B., Borga, M., Brázdil, Claps, P., Kiss, A., Kjeldsen, T.R., Kriaučiunienė, J., Kundzewicz, Z. W., Lang, M., Llasat, M.C., Macdonald, N., McIntyre, N., Mediero, L., Merz, B., Merz, R., Molnar, P., Montanari, A., Neuhold, C., Parajka, J., Perdigão, R.A.P., Plavcová, L., Rogger, M., Salinas, J.L., Sauquet, E., Schär, C., Szolgay, J., Viglione, A., Blöschl, G. (2014): Un-derstanding flood regime changes in Europe: a state-of-the-art assessment, Hydrol. Earth Syst. Sci., 18, 2735 – 2772, doi: 10.5194/hess-18-2735-2014

Katz, R.W., and Glantz, M. H. (1986): Anatomy of a rainfall index. Mon.Wea. Rev., 114, 764-771.

Kiem, A. S., Franks, S. W., and Kuczera, G. (2003), Multi-decadal variability of flood risk, Geophys. Res. Lett., 30, 1035, doi:10.1029/2002GL015992, 2.

Klein, B. (2009: Ermittlung von Ganglinien für die risikoorientierte Hochwasserbemessung von Talsperren. Dissertation, University of Bochum, Germany, 205 p.

Lang, M., Ouarda, T.B.M.J., Bobée, B., 1999. Towards operational guidelines for overthreshold modelling. J. Hydrol. 225 (1999), 103–117.LAWA(1997): Pegelvorschrift-Stammtext. Kulturbuchverlag Berlin GmbH, Berlin.

Lindström, G. and S. Bergström (2004). Runoff trends in Sweden 1807-2002. Hydrological Sciences Journal-Journal Des Sciences Hydrologiques 49(1): 69-83.

Llasat, M.-C., Barriendos, M., Barrera, A., Rido, T. (2005): Floods in Catalonia (NE Spain) since the 14th century. Climatological and meteorological aspects from historical documentary sources and old instrumental records. J. Hydrol., 313, 32 – 47, doi: 10.1016/j.jhydrol.2005.02.004.

Longobardi, A., Villani, P., Grayson, R. B., and Western, A. W. (2003): On the relationship between runoff coefficient and catchment initial conditions, in Proceedings of the International Congress on Modelling and Simulation, vol. 2, pp. 867–872, Modell. and Simul. Soc. of Australia and New Zealand, Townsville, Australia.

McCabe, G. J. and Wolock, D. M. (2002): A step increase in streamflow in the conterminous United States. Geophysical Research Letters 29: 38-31 - 38-34.

Mediero, L., Kjeldsen, T.R., Macdonald, N., Kohnova, S., Merz, B., Vorogushyn, S., Wilson, D., Alburquerque, T., Blöschl, G., Bogdanowicz, E., Castellarin, A., Hall, J., Kobold, M., Kriauciuni-ene,J., Lang, M., Madsen, H., Onuşluel Gül, G., Perdigão, R.A.P., Roald, L.A., Salinas, J.L., Toumazis, A.D.,Veijalainen, N., Þórarinsson, Ó. (2015): Identification of coherent flood regions across Europe by using the longest streamflow records, Journal of Hydrology 528, 341 – 360, doi: http://dx.doi.org/10.1016/j.jhydrol.2015.06.016

Merz, B., Nguyen, V. D., Vorogushyn, S. (2016): Temporal clustering of floods in Germany: Do flood-rich and flood-poor periods exist? J. Hydrol., 541, 824 – 838, doi: 10.1016/j.jhydrol.2016.07.041.

Merz, R., Blöschl, G. (2009): A regional analysis of event runoff coefficients with respect to climate and catchment characteristics, Water Resour. Res., 45, W01405, doi:10.1029/2008WR007163.

Moron, V., Robertson, A.W., Ward, M.N. (2006): Seasonal Predictability and Spatial Coherence of Rainfall Characteristics in the Tropical Setting of Senegal. Mon. Wea. Rev., 134, 3248–3262, doi: 10.1175/MWR3252.1.

Moron, V., Robertson, A. W., Ward, M. N., and Camberlin, P. (2007): Spatial Coherence of Tropical Rainfall at the Regional Scale. J. Climate, 20, 5244–5263, doi: 10.1175/2007JCLI1623.1.

Mudelsee, M., Börngen, M., Tetzlaff, G. and Grünewald, U. (2004): Extreme floods in central Europe over the past 500 years: role of cyclone pathway „Zugstrasse Vb". J. Geophys. Res., 109 (D23), D23101, doi: 10.1029/2004JD005034

Mudelsee, M., Deutsch, M., Börngen, M., and Tetzlaff, G. (2006): Trends in flood risk oft he River Werra (Germany) over the past 500 years. Hydrol. Sci. J., 51, 818 – 833.

Nied, M., Pardowitz, T., Nissen, K., Ulbrich, U., Hundecha, Y., Merz, B. (2014): On the relationship between hydro-meteorological patterns and flood tipes. J. Hydrol., 519, 3249 – 3262, 10.1016/j.jhydrol.2014.09.089

Oppenheim, A.V., Schafer, R.W., and Buck, J.R. (1999): Discrete-time signal processing. Upper Saddle River, NJ: Prentice Hall.

Österle H., Werner P.-C., Gerstengarbe F.-W. (2006): Qualitätsprüfung, Ergänzung und Homogenisierung der täglichen Datenreihen in Deutschland, 1951-2003: ein neuer Datensatz. http://www.meteo.physik.uni-muenchen.de/dkt/poster.html . /7. Deutsche Klimatagung/, Klimatrends: Vergangenheit und Zukunft, 9. - 11 Oktober 2006, München

Österle H. (2001): Reconstruction of daily global radiation for past years for use in agricultural models, Physics and Chemistry of the Earth, Part B: Hydrology, Oceans and Atmosphere, 26(3), 253–256.

Petrow, T., Merz, B., Lindenschmidt, K.-E., Thieken, A.H. (2007): Aspects of seasonality and flood generating circulation patterns in a mountainous catchment in south-eastern Germany. Hydrol. Earth Syst. Sci., 11, 1455–1468

Petrow, T., Zimmer, J., Merz, B. (2009): Changes in the flood hazard in Germany through changing frequency and persistence of circulation patterns. Nat. Haz. Earth Syst Scie (NHESS), 9, 1409 – 1423, www.nat-hazards-earth-syst-sci.net/9/1409/2009

Plate, E. J.,Ihringer, J., Lutz, W. (1988): Operational models for flood calculations, J. Hydrol., Volume 100, Issue 1, Pages 489-506, ISSN 0022-1694, http://dx.doi.org/10.1016/0022-1694(88)90198-9.

(http://www.sciencedirect.com/science/article/pii/0022169488901989)

Poli, P., Hersbach, H., Dee, D., Berrisford, P., Simmons, A., Vitart, F., Laloyaux, P., Tan, D., Peubey, C., Thépaut, J., Trémolet, Y., Hólm, E., Bonavita, M., Isaksen, L., and Fisher, M., (2016): ERA-20C: An Atmospheric Reanalysis of the Twentieth Century. J. Climate, 29, 4083–4097, doi: 10.1175/JCLI-D-15-0556.1.

Robson, A. J. (2002): Evidence for trends in UK flooding. Phil.Trans.Soc Lond A, 360, 1327-1343.

Schmocker-Fackel, P. and Naef, F. (2010a): More frequent flooding? Changes in flood frequency in Switzerland since 1850. J. Hydrol, 381, 1 – 8, doi: 10.1016/jhydrol.2009.09.022

Schmocker-Fackel, P. and Naef, F. (2010b): Changes in flood frequencies in Switzerland since 1500. Hydrol. Earth Syst. Sci., 14, 1581–1594, doi: 10.5194/hess-14-1581-2010

Steirou, E.-S., Gerlitz, L., Apel, H., Merz, B. (2017): Links between large-scale circulation patterns and streamflow in Central Europe: A review. - Journal of Hydrology, 549, pp. 484—500, http://doi.org/10.1016/j.jhydrol.2017.04.003

Uhlemann, S., Thieken, A. H., and Merz, B. (2010): A consistent set of trans-basin floods in Germany between 1952 – 2002, Hydrol. Earth Syst. Sci., 14, 1277-1295, doi: 10.5194/hess-14-1277-2010.

USWRC (1976): Guidelines for Determining Flood Flow Frequency, Bulletin No. 17. U.S. Water Resources Council, Subcommittee on Hydrology, Washington, D.C.

Ward, P.J., Beets, W., Bouwer, L.M., Aerts, J.C.J.H., Renssen, H. (2010). Sensitivity of river discharge to ENSO. Geophysical Research Letters, 37(12), L12402.

Ward, P. J., Eisner, S., Flörke, M., Dettinger, M. D., Kummu, M. (2014). Annual flood sensitivities to El Niño–Southern Oscillation at the global scale, Hydrol. Earth Syst. Sci., 18, 47-66, https://doi.org/10.5194/hess-18-47-2014.

Supplement

Table S1: Main characteristics of selected gauges. Flood regime according to Figure 3. Gauges in bold are those shown in Figure 1.

#	Gauge name	River	Basin	Cat. area [km^2]	Specific mean flow [$m^3 s^{-1} km^{-2}$]	Flood Regime	Location	
							Lat	Long
1	Achstetten	B. Rot	Danube	264	0.0125	C	48.26	9.9
2	Kempten	Iller	Danube	955	0.0491	B	47.73	10.32
3	Fuerstenfeldbruck	Amper	Danube	1235	0.0191	B	48.18	11.26
4	Beuron	Donau	Danube	1309	0.0087	A	48.05	8.97
5	Chamerau	Regen	Danube	1357	0.0192	C	49.18	12.75
6	Seebruck	Alz	Danube	1388	0.0373	B	47.94	12.48
7	Eichstaett	Altmuehl	Danube	1400	0.0071	A	48.88	11.2
8	Landsberg	Lech	Danube	2295	0.0358	B	48.04	10.88
9	Regenstauf	Regen	Danube	2658	0.0141	A	49.13	12.13
10	Muenchshofen	Naab	Danube	4014	0.0093	A	49.24	12.08
11	Heitzenhofen	Naab	Danube	5426	0.0090	A	49.12	11.94
12	**Burghausen**	**Salzach**	**Danube**	**6649**	**0.0377**	**B**	**48.16**	**12.84**
13	Landau	Isar	Danube	8467	0.0200	B	48.68	12.69
14	Plattling	Isar	Danube	8839	0.0198	B	48.77	12.88
15	Oberaudorf	Inn	Danube	9712	0.0314	B	47.65	12.2
16	Dillingen	Donau	Danube	11315	0.0143	C	48.57	10.5
17	Wasserburg	Inn	Danube	11980	0.0296	B	48.06	12.23
18	Eschelbach	Inn	Danube	13354	0.0278	B	48.26	12.73
19	Donauwoerth	Donau	Danube	15037	0.0127	C	48.71	10.8
20	Ingolstadt	Donau	Danube	20001	0.0157	C	48.76	11.42
21	Kelheim	Donau	Danube	22950	0.0145	C	48.92	11.87
22	Passau-Ingling	Inn	Danube	26084	0.0283	B	48.56	13.44
23	Oberndorf	Donau	Danube	26446	0.0134	C	48.95	12.02
24	Hofkirchen	Donau	Danube	47496	0.0136	C	48.68	13.12
25	**Achleiten**	**Donau**	**Danube**	**76653**	**0.0186**	**B**	**48.58**	**13.51**
26	Wegeleben	Bode	Elbe	1215	0.0069	A	51.89	11.19
27	Greiz	W. Elster	Elbe	1255	0.0084	C	50.66	12.2
28	Lichtenwalde	Zschopau	Elbe	1575	0.0138	C	50.89	13.02
29	Wechselburg	Z. Mulde	Elbe	2107	0.0126	C	51.01	12.77
30	Hadmersleben	Bode	Elbe	2758	0.0051	A	52.01	11.32
31	Camburg-Stoeben	Saale	Elbe	3977	0.0079	C	51.07	11.7
32	Oldisleben	Unstrut	Elbe	4174	0.0045	A	51.3	11.18
33	Golzern	V. Mulde	Elbe	5442	0.0114	C	51.25	12.78
34	Calbe	Saale	Elbe	23719	0.0048	C	51.92	11.81

35	**Dresden**	**Elbe**	**Elbe**	**53096**	**0.0061**	**C**	**51.06**	**13.74**
36	Barby	Elbe	Elbe	94060	0.0059	C	51.99	11.88
37	Magdeburg	Elbe	Elbe	94942	0.0059	C	52.14	11.65
38	**Wittenberge**	**Elbe**	**Elbe**	**123532**	**0.0047**	**C**	**52.99**	**11.75**
39	Neu-Darchau	Elbe	Elbe	131950	0.0056	C	53.23	10.89
40	Rheine	Ems	Ems	3740	0.0054	A	52.29	7.43
41	Hohensaaten-Finow	Oder	Oder	109564	0.0096	C	52.87	14.14
42	Altensteig	Nagold	Rhein	135	0.0194	A	48.58	8.61
43	Bad-Imnau	Eyach	Rhein	331	0.0093	C	48.41	8.77
44	Pforzheim-Wuerm	Wuerm	Rhein	418	0.0070	C	48.87	8.71
45	Schwaibach	Kinzig	Rhein	954	0.0241	A	48.39	8.03
46	Doerzbach	Jagst	Rhein	1030	0.0098	A	49.37	9.72
47	Nuernberg	Pegnitz	Rhein	1192	0.0093	A	49.46	11.05
48	Tauberbischofsheim	Tauber	Rhein	1584	0.0055	A	49.63	9.67
49	Bad-Kissingen	F. Saale	Rhein	1587	0.0076	A	50.18	10.07
50	Kesseler3	Lippe	Rhein	2003	0.0118	A	51.66	8.09
51	Plochingen	Neckar	Rhein	3995	0.0120	A	48.71	9.42
52	Pettstadt	Pegnitz	Rhein	7005	0.0075	A	49.84	10.94
53	**Neuhausen**	**Rhein**	**Rhein**	**11887**	**0.0310**	**B**	**47.68**	**8.63**
54	**Schweinfurt**	**Main**	**Rhein**	**12715**	**0.0082**	**A**	**50.03**	**10.22**
55	Rekingen	Rhein	Rhein	14718	0.0299	B	47.57	8.33
56	**Cochem**	**Mosel**	**Rhein**	**27088**	**0.0116**	**A**	**50.14**	**7.17**
57	Maxau	Rhein	Rhein	50196	0.0250	C	49.04	8.31
58	Kaub	Rhein	Rhein	103488	0.0159	A	50.09	7.77
59	**Cologne**	**Rhein**	**Rhein**	**144232**	**0.0146**	**A**	**50.94**	**6.96**
60	Meiningen	Werra	Weser	1170	0.0121	A	50.58	10.42
61	Schmittlotheim	Eder	Weser	1202	0.0158	A	51.16	8.9
62	Gross-Schwuelper	Oker	Weser	1734	0.0066	A	52.35	10.43
63	Rotenburg	Fulda	Weser	2523	0.0086	A	51.01	9.72
64	Gerstungen	Werra	Weser	3039	0.0102	A	50.96	10.07
65	Celle	Aller	Weser	4128	0.0065	A	52.62	10.06
66	Guntershausen	Fulda	Weser	6366	0.0089	A	51.23	9.47
67	Hann.-Muenden	Weser	Weser	12442	0.0090	A	51.43	9.64
68	**Vlotho**	**Weser**	**Weser**	**17618**	**0.0094**	**A**	**52.18**	**8.86**

Figure S1: Flood events and AMS values for the 68 catchments for each hydrological year 1932-2005. The years are ordered according to the event-type indicator, from event-type years to non-event-type years. Horizontal axis shows the day of the year, vertical axis the AMS magnitude (standardized). Vertical lines indicate an event with at least one AMS occurrence. Different colors indicate the flood regimes (Green: Region A; Red: Region B; Blue: Region C), different symbols correspond to different flood events. Abbreviations: *n*: number of flood events; *EI*: event-type indicator; *sdQ*: indicator of magnitude coherence, i.e. standard deviation of 68 AMS magnitudes (standardized); *mQ*: mean of 68 AMS magnitudes (standardized).

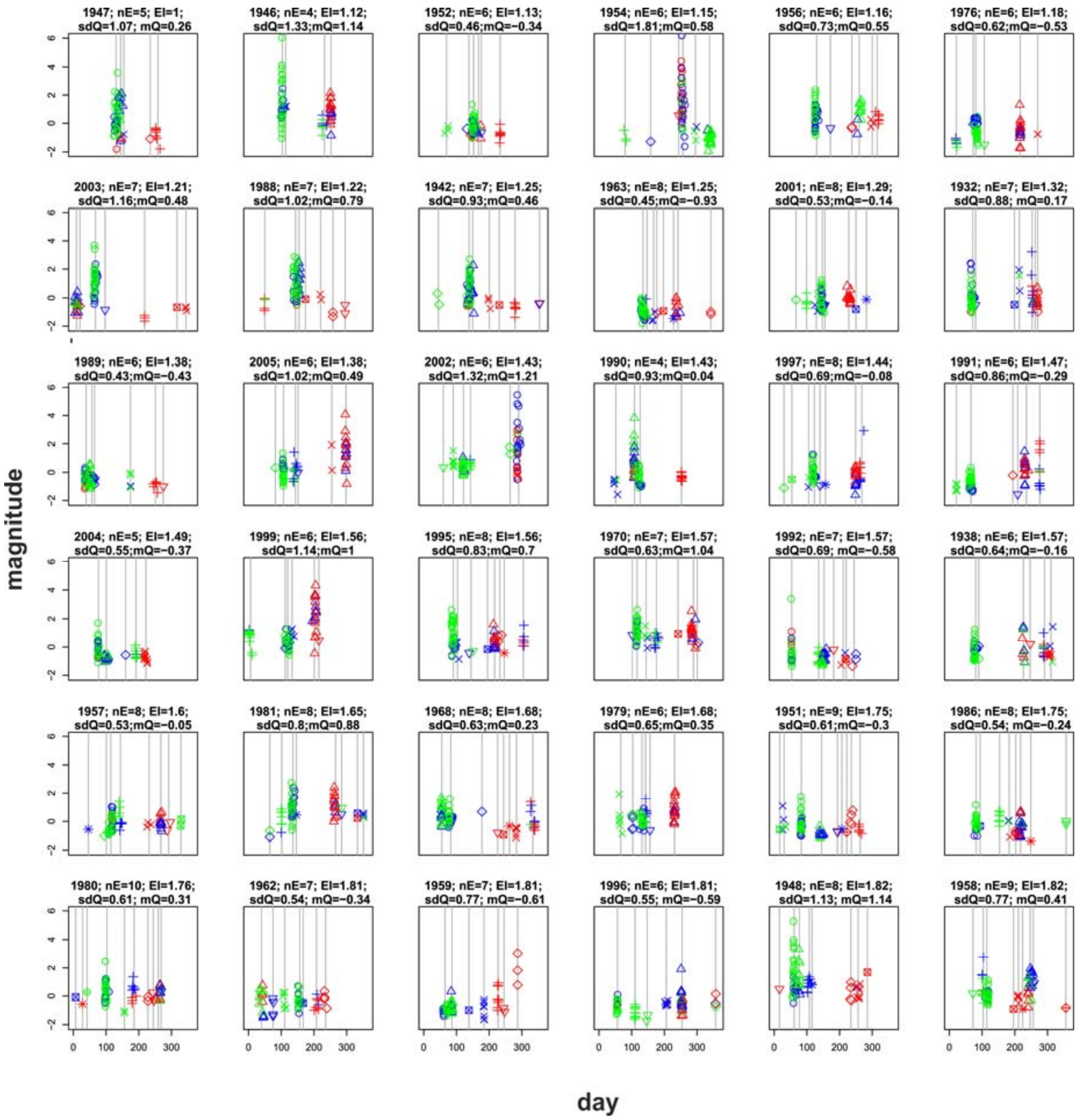

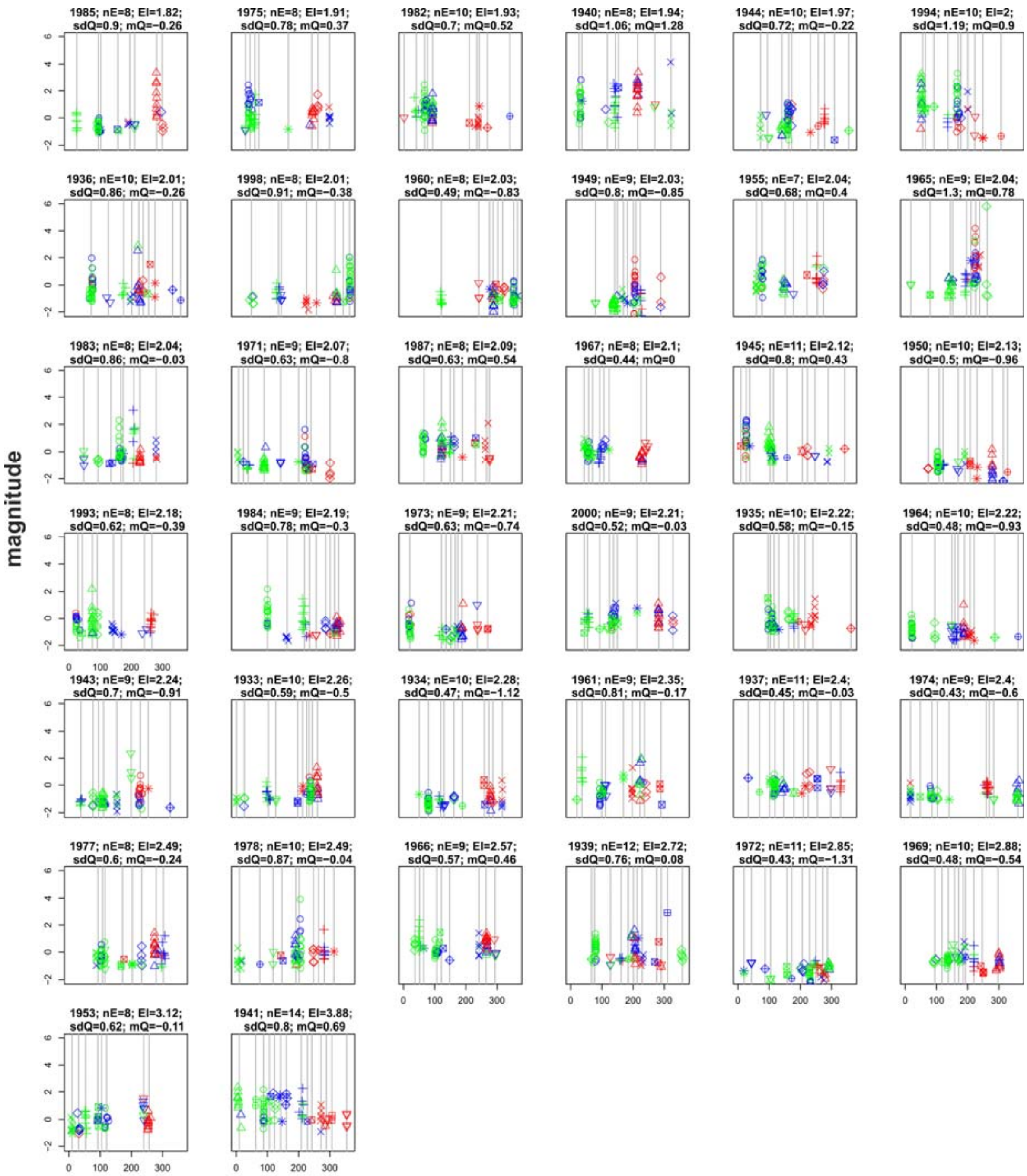

933

934